

Viscosity and drag force involved in organelle transport: Investigation of the fluctuation dissipation theorem*

K. Hayashi^{1,a}, C.G. Pack², M.K. Sato³, K. Mouri², K. Kaizu⁴, K. Takahashi^{4,5}, and Y. Okada⁴

¹ School of Engineering, Tohoku University, Sendai, Japan

² Cellular Informatics Lab, RIKEN, Wako, Japan

³ Institute of Multidisciplinary Research for Advanced Material Tohoku University, Sendai, Japan

⁴ Quantitative Biology Center, RIKEN, Suita, Japan

⁵ Institute for Advanced Biosciences, Keio University, Fujisawa, Japan

Received 21 July 2013 and Received in final form 22 October 2013

Published online: 4 December 2013 – © EDP Sciences / Società Italiana di Fisica / Springer-Verlag 2013

Abstract. We observed the motion of an organelle transported by motor proteins in cells using fluorescence microscopy. Particularly, among organelles, the mitochondria in PC12 cells were studied. A mitochondrion was dragged at a constant speed for several seconds without pausing. We investigated the fluctuation dissipation theorem for this constant drag motion by comparing it with the motion of Brownian beads that were incorporated into the cells by an electroporation method. We estimated the viscosity value inside cells from the diffusion coefficients of the beads. Then the viscosity value obtained by using the beads was found to be slightly lower than that obtained from the diffusion coefficient for the organelle motion via the Einstein relation. This discrepancy indicates the violation of the Einstein relation for the organelle motion.

1 Introduction

The fluctuation dissipation theorem (FDT), the fluctuation theorem (FT) and their several important consequences have been used in biological systems recently to investigate their energetic properties [1–12]. For example, the Jarzynski equality and the Crooks fluctuation theorem are useful in computing the free energy difference between two equilibrium states and have been experimentally tested in single RNA/DNA hairpin systems [4–6]. Another kind of the FT has been suggested as being useful for measuring the forces of motor proteins [7–12].

In this present study, we investigated diffusion properties and the FDT for organelle motion in a living cell that a 1 μm sized organelle was transported by motor proteins traveling along microtubules in a cell (fig. 1(a)) [13]. The motion of organelles includes movements and pauses. Typically organelles were dragged for several seconds without pausing. While subdiffusive behavior has been reported for the motion of organelles, including complex dynamics, such as movements and pauses [14], diffusion appeared normal when we focused only on motion at a constant speed. Although the fluctuation properties for the complex motion of organelles are often studied, those for the con-

stant drag motion have been less focused on. Investigation of this non-equilibrium steady state is important because drag force acting on an organelle may provide information to elucidate the mechanism of organelle transport by multiple motors.

We measured the diffusion coefficient for the constant drag motion of an organelle, and compared it with the diffusion coefficients of Brownian beads incorporated into cells by an electroporation method. These beads were assumed to diffuse in the cells mainly due to thermal noise. The viscosity values were estimated from the diffusion coefficients of the beads by using the Einstein relation. Because the large molecules interacted with vesicles and filaments as well as with proteins, the viscosity value obtained by using 1 μm sized beads was much higher than the viscosity of cytosol. Then this value was compared with that estimated from the diffusion coefficient of transported organelles using the Einstein relation. The former was found to be slightly lower than the latter. The discrepancy indicates the violation of the Einstein relation for the organelle motion.

2 Fluorescence observation

We experimentally observed the mitochondria in PC12 cells (fig. 1(b)). PC12, a cell line derived from rat pheochromocytoma, has been widely used as a model system for neuronal differentiation [15]. We chose to

* Supplementary material in the form of four .avi files and a .pdf file available from the Journal web page at <http://dx.doi.org/10.1140/epje/i2013-13136-6>

^a e-mail: kumiko@camp.apph.tohoku.ac.jp

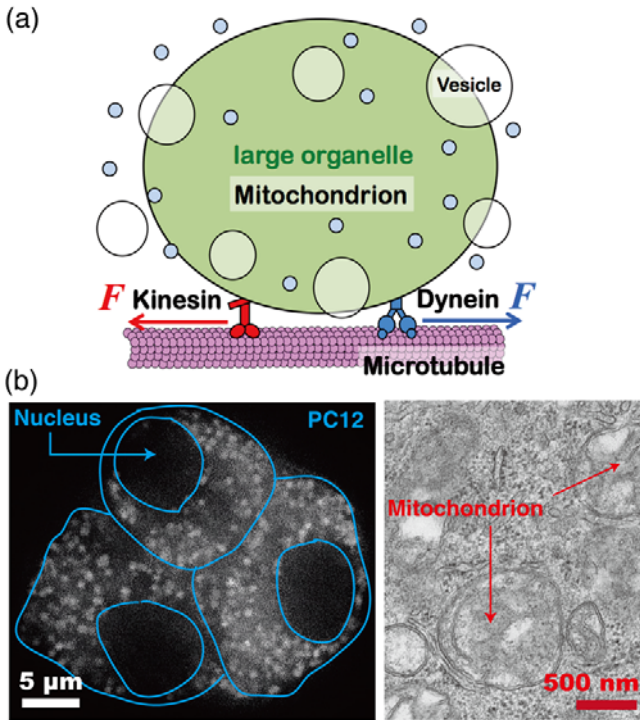


Fig. 1. (a) Schematic of mitochondrial transport (not to scale). The sizes of the organelle and the motors are approximately $1\ \mu\text{m}$ and $10\ \text{nm}$, respectively. (b) Fluorescence microscopy of PC12 cells; each bright, round spot represents a mitochondrion (left). A representative image of mitochondria in a PC12 cell observed by transmission electron microscopy (see *Method* in Supplementary Material) (right).

study mitochondria because they can be brightly and selectively stained with an organic fluorescent dye, tetramethylrhodamine ethyl ester (see *Method* in Supplementary Material). The shape of a mitochondrion varies considerably among different types of cells. They normally take an elongated tubular shape but in various sizes. Interestingly, however, they took similar oblong shapes in the differentiating PC12 cells, as shown in the fluorescence images (fig. 1(b), left) and the electron micrographs (fig. 1(b), right). Mitochondria observed in PC12 cells were transported by motor proteins along microtubules for several seconds without pausing (see Supplementary Movies). During these time intervals, large changes in mitochondrial shapes were not observed. The position $X(t)$ of the center of a mitochondrion was calculated from the recorded images. Figure 2(a) shows the trajectories obtained for approximately 350 mitochondria from 48 different cells with velocities v ranging from approximately 200 to $1500\ \text{nm/s}$. The trajectories were identified between long pauses ($\sim 1\ \text{s}$) (fig. 3(a), inset). Note that in fig. 3(a), movement in all directions is represented along the x -axis, which is the direction of microtubules. The microtubules were considered to be straight for several micron length (fig. 2).

For $X(t)$ as shown in fig. 3(a), whose length is longer than $1.5\ \text{s}$, we calculated the power spectrum $S(\nu)$ defined

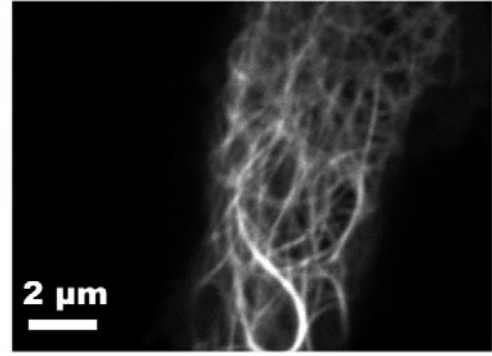


Fig. 2. Fluorescence observation of microtubules in the cells (see *Method* in Supplementary Material). The white curves were microtubules. The microtubules were considered to be straight for several micron length. Intervals between microtubules were about $1.5\ \mu\text{m}$.

by

$$S(\nu) = \frac{\langle |\hat{X}_\nu|^2 \rangle}{\tau}, \quad \hat{X}_\nu = \int_{-\tau/2}^{+\tau/2} X(t) e^{-i2\pi\nu t} dt, \quad (1)$$

where $\tau = N_w/23\ \text{s}$ (note that the recording rate was 23 frames/s), N_w is the window size and $\langle \cdot \rangle$ denotes the time average over the trajectory. In fig. 3(b) (top), normal diffusive behavior ($S(\nu) \propto \nu^{-2}$) was observed for small ν . (Note that the behavior of $S(\nu)$ for large ν was considered to be a numerical artifact, see sect. IC of Supplementary Material.) While subdiffusive behavior has been reported for the motion of a different organelle, including complex dynamics, such as movements and pauses [14], diffusion appeared normal when we focused only on motion at a constant speed, noting that diffusion became abnormal when the trajectories included pauses and reversals (fig. 3(b), bottom). The normal diffusive behavior ($S(\nu) \propto \nu^{-2}$) for small ν indicated that for the large scale behavior of $X(t)$ can be phenomenologically described by

$$\frac{dX}{dt} = v + \sqrt{2D_m} \xi(t), \quad (2)$$

where ξ is Gaussian noise with a variance equal to 1.

The value of the diffusion coefficient D_m of a mitochondrion was determined as follows: We divided the trajectories $X(t)$ shown in fig. 3(a) into 10 groups according to the velocity values (in nanometers per second) of the mitochondria as follows: $200 < v \leq 300$; $300 < v \leq 400$; $400 < v \leq 500$; $500 < v \leq 600$; $600 < v \leq 700$; $700 < v \leq 800$; $800 < v \leq 900$; $900 < v \leq 1000$; $1000 < v \leq 1200$; $1200 < v \leq 1500$. Ideally, D_m of each mitochondrion should be estimated using the trajectory of one mitochondrion; however, we could not obtain a sufficiently long measurement of $X(t)$ from one mitochondrion to accurately calculate D_m , because mitochondria in PC12 cells often stopped after moving for several seconds. Instead, we obtained an approximate value of D_m from trajectories of different mitochondria for each group, setting

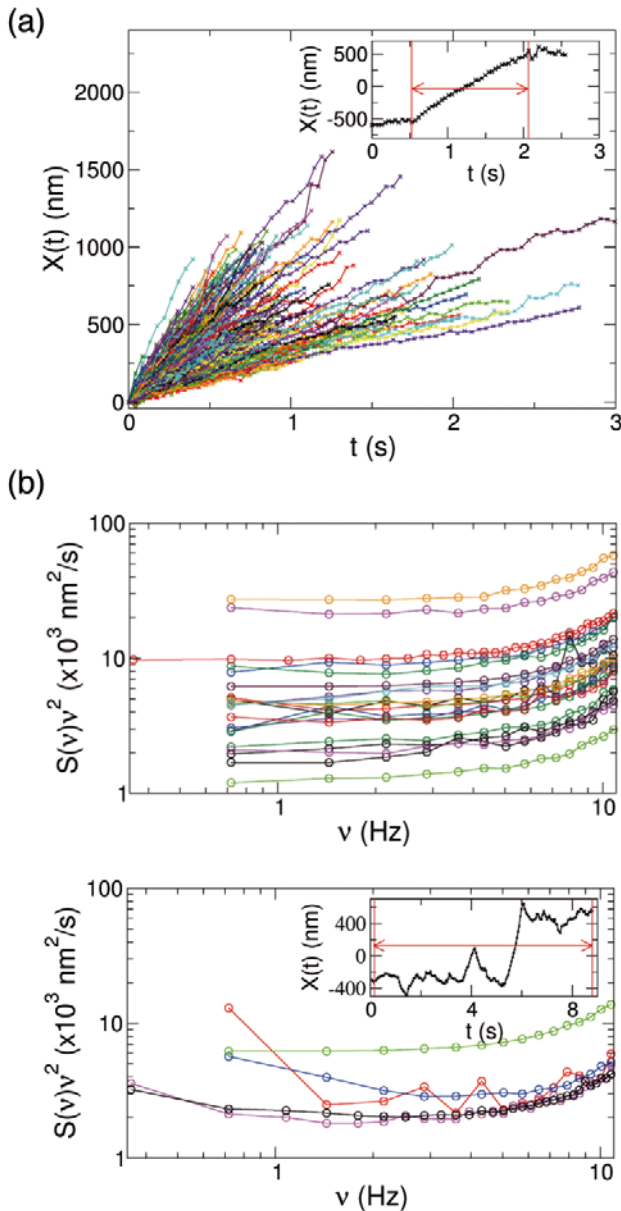


Fig. 3. (a) The trajectories $X(t)$, which were identified between long pauses (inset), of approximately 350 mitochondria from 48 cells. The recording rate was 23 frames/s. (b) The power spectrum $S(\nu)$ calculated using $X(t)$, shown in (a), whose length is longer than 1.5 s, with a window size $N_w = 2^5$ or 2^6 (top). Here we plot $S(\nu)\nu^2$ as a function of ν to see clearly $S(\nu) \propto \nu^{-2}$ for small ν . On the other hand, $S(\nu)$ calculated using the trajectories that include pauses and reversals (bottom, inset: an example of such trajectories), was not $\propto \nu^{-2}$ (bottom).

the velocity range to less than $\sqrt{2D_m}$ (then grouping different trajectories was considered not to affect on velocity fluctuation much). To estimate D_m , for each group, we calculated the probability distribution $P(\Delta X)$, where $\Delta X = X(t + \Delta t) - X(t)$. Figure 4(a) shows the values of $P(\Delta X)$ for $\Delta t = 43, 87, 130,$ and 174 ms for the velocity range of 900–1000 nm/s (for the complete results

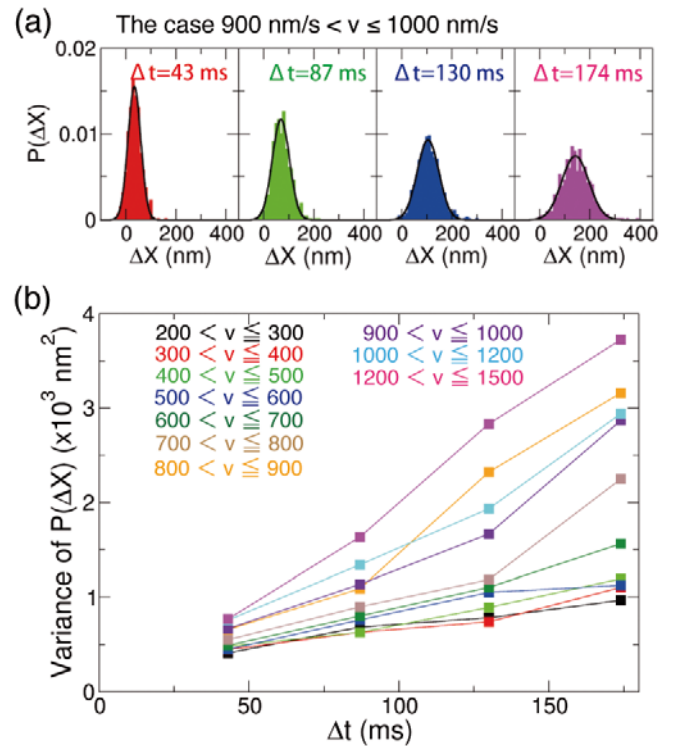


Fig. 4. (a) Plot of $P(\Delta X)$, where $\Delta X = X(t + \Delta t) - X(t)$ ($X(t)$ is a trajectory shown in fig. 3(a)) fitted using a Gaussian function $\exp(-(\Delta X - b)^2/2a)/\sqrt{2\pi a}$ (the black curves), where a and b are fitting parameters for the velocity range of 900–1000 nm/s (for the complete results for the 10 groups, see fig. S4 of Supplementary Material). (b) The variance a ($= \langle (\Delta X - \langle \Delta X \rangle_s)^2 \rangle_s$) of $P(\Delta X)$ is plotted as a function of Δt . Here $\langle \cdot \rangle_s$ denotes a sample average. Each color represents the group classified according to the velocity values (in nanometers per second) of $X(t)$ shown in fig. 3(a).

for the 10 groups, see fig. S4 of Supplementary Material). Each $P(\Delta X)$ was well described by a Gaussian function $\exp(-(\Delta X - b)^2/2a)/\sqrt{2\pi a}$ (black curves in fig. 4(a)), where a ($= \langle (\Delta X - \langle \Delta X \rangle_s)^2 \rangle_s$) and b ($= \langle \Delta X \rangle_s$) are fitting parameters (here $\langle \cdot \rangle_s$ denotes a sample average). Then, D_m was defined as $a/2\Delta t$, and the value of $a/\Delta t$ was obtained by the fitting of the graph in fig. 4(b).

3 Fluctuation dissipation theorem

In the fluctuation dissipation theorem (FDT), a friction coefficient is a significant quantity in statistical mechanics as well as a diffusion coefficient. Because the friction coefficient Γ_m of a mitochondrion can be approximated by $\Gamma_m = 6\pi\eta r_m$ with a shape approximated by a sphere having the radius r_m , we were able to investigate Γ_m based on the fluorescence intensity of a mitochondrion, which is proportional to r_m . Here, η is the viscosity of medium. Note that we cannot measure the sizes of mitochondria (r_m) in the cells because the fluorescent images were not clear enough to measure their diameters accurately (see the inset in fig. 5). Figure 5 shows that the fluorescence

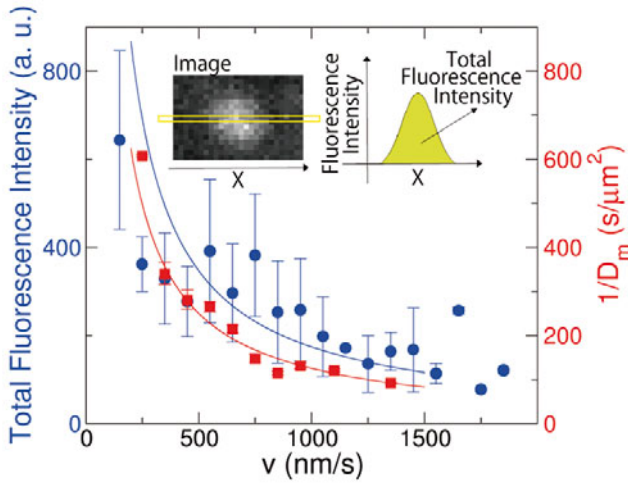


Fig. 5. Total fluorescence intensity (blue) and diffusion coefficients D_m (red) of mitochondria plotted as a function of velocity. The blue line shows the total fluorescence intensity $= a_f/v$ where $a_f = 2.0 \times 10^5$, and the red line shows $1/D_m = a_D/v$ where $a_D = 1.0 \times 10^5$. Regarding the calculation of the total fluorescence intensity, we first measured the fluorescence intensity of an mitochondrion along X -direction (the yellow rectangle in the inset (left)). Then total fluorescence intensity, which is the yellow area in the inset (right), was calculated. On the other hand, D_m was measured from the variance of $P(\Delta X)$ shown in fig. 4(a). The error bars of the fluorescence intensity (blue) represent the standard deviations over different mitochondria, and the error bars of D_m (red) represent the fitting errors when the values of $a/\Delta t$ were obtained by the fitting of the graphs in fig. 4(b).

intensity is inversely proportional to v . This indicates that the velocity of a mitochondrion depends on the size, and $\Gamma_m = 6\pi\eta r_m \propto v^{-1}$. Note that an *in vitro* assay of kinesin revealed that a viscous load was $\propto v^{-1}$ when the viscosity of the buffer was increased until it was 60 times that of water [16], while v did not depend on a viscous load in the low-viscosity solution because the time for motor proteins to hydrolyze ATP was slower than the diffusion time of a probe attached to motor proteins. $\Gamma_m \propto v^{-1}$ was observed in the cells because the viscosity of the medium surrounding a $1 \mu\text{m}$ sized organelle, which includes that of the cytosol and reflects interactions with other organelles, macromolecular complexes, and cytoskeletal components, may be large.

The facts that $D_m \propto v$ and $\Gamma_m \propto v^{-1}$ seen in fig. 5 suggest that $D_m \propto 1/\Gamma_m$. There is an inverse proportional relationship of the fluctuation D_m and the dissipation Γ_m based on the Einstein relation, which is a kind of the FDT, $D_m = k_B T / \Gamma_m$ (k_B is the Boltzmann constant and T is the temperature of the environment). We attempted to determine as to what extent the Einstein relation was violated in the non-equilibrium steady state. We note that for another biological system (myosin filaments in actin filaments), the violation of the fluctuation response relation was of an order of magnitude [2].

In order to check the Einstein relation for the organelle motion, we compared the organelle motion with the mo-

Table 1. Diffusion coefficient ($\mu\text{m}^2/\text{s}$) for green fluorescent protein (GFP), fluorescent beads (FB) and fluorescent nanodiamond (FD) obtained from FCS measurements. The diameters of the probes are indicated by d . The error bars represent the standard deviations over different cells. The values of $20 \mu\text{m}$ sized PC12 cells were compared with those of $100 \mu\text{m}$ sized HeLa cells. The values without citations were obtained in the present study.

probe	PC12 cells	HeLa cells
GFP ($d = 4 \text{ nm}$)	23 ± 4.0	24 ± 3.5 [18]
FB ($d = 60 \text{ nm}$)	0.85 ± 0.4	1.0 ± 0.5 [18]
FD ($d = 150 \text{ nm}$)	no data	0.08 [20]
FB ($d = 320 \text{ nm}$)	0.046 ± 0.023	no data
FB ($d = 460 \text{ nm}$)	0.038 ± 0.022	0.030 ± 0.024

tion of Brownian beads (fluorescent beads) incorporated into the PC12 cells by an electroporation method. The sizes of the beads were similar to those of mitochondria. Using fluorescence correlation spectroscopy (FCS) measurement of the beads, we estimated the viscosity values (η_{FCS}) of the surrounding medium to be $\eta_{\text{FCS}} = 2\text{--}4 \times 10^{-8} \text{ pN s/nm}^2$ (20–40 times the viscosity of water). (In the following section, we explained about the FCS measurement in detail.) On the other hand, when we estimated the viscosity (η_{ER}) by applying the Einstein relation to the organelle motion, we obtained $\eta_{\text{ER}} = 6 \times 10^{-8} \text{ pN s/nm}^2$ (60 times the viscosity of water). Here we substituted $\langle r_m \rangle_s = 400 \text{ nm}$ (S.D. = 100 nm) obtained by the transmission electron microscopy measurements (fig. 1(b), right), $D_m = 0.009 \mu\text{m}^2/\text{s}$ at $\langle v \rangle_s = 900 \text{ nm/s}$ and $T = 37^\circ\text{C}$, into $D_m = k_B T / 6\pi\eta_{\text{ER}} \langle r_m \rangle_s$. By comparing η_{ER} with the real viscosity value η_{FCS} , we found that the extent of violation of the Einstein relation for the organelle motion was about 2 ($\sim \eta_{\text{ER}}/\eta_{\text{FCS}}$).

4 Fluorescence correlation spectroscopy (FCS)

FCS is the measurement method that dynamic properties, such as a diffusion coefficient, of fluorescent molecules in cells are obtained from their fluorescence intensity, and attracts attention in the fields of cell biology and biophysics. To estimate the viscosity of the intracellular medium of PC12 cells, we measured the diffusion coefficients D of different fluorescent probes (table 1) by using FCS (see *Method* in Supplementary Material) [17, 18]. In our FCS experiment, the fluorescent probes were taken in the cells as follows: Green fluorescent proteins (GFPs) were expressed in the cells, and fluorescent beads were incorporated into the cells using an electroporation method (fig. 6(a) for 460 nm sized beads).

Figure 6(b) (inset) shows a plot of $I(t)$, which is the fluorescence intensity of 460 nm sized beads diffusing in a PC12 cell. Using $I(t)$, the autocorrelation function $g(\tau)$

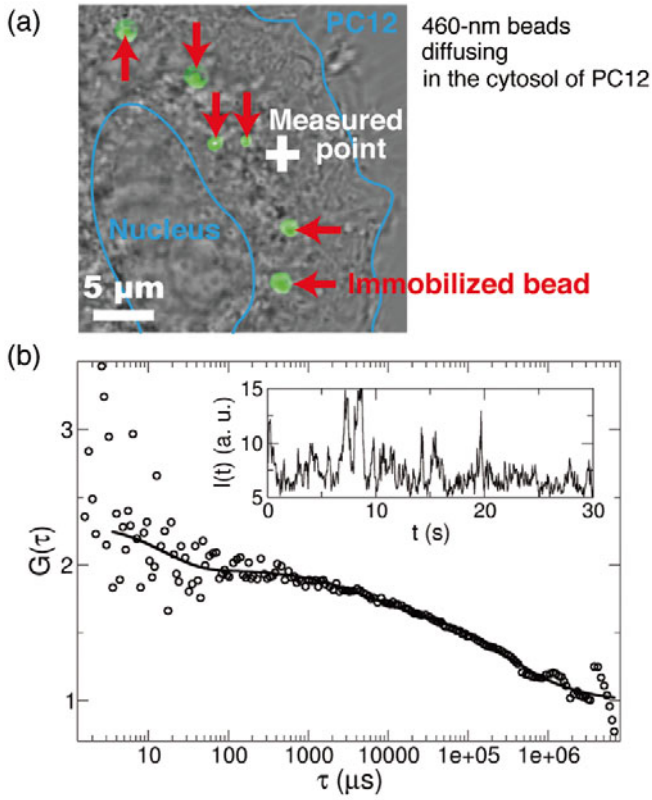


Fig. 6. (a) A PC12 cell after electroporation with 460 nm sized fluorescent beads. The measured point with FCS (a plus symbol) and the immobilized beads (red arrows) are indicated. (b) FCS measurement result of the autocorrelation function $G(\tau)$ defined by eq. (4) (open circles), where $I(t)$ is the fluorescence intensity (inset). From the fitting function (solid curve described by eq. (5)), we obtained the diffusion coefficient D ($= 0.04 \pm 0.02 \mu\text{m}^2/\text{s}$) for the 460 nm sized beads.

was calculated as

$$g(\tau) = \frac{\langle I(t)I(t+\tau) \rangle}{\langle I \rangle^2}, \quad (3)$$

where $\langle \cdot \rangle$ denotes a time average. Note that in fig. 6(b), we plotted $G(\tau)$, where

$$G(\tau) = \frac{g(\tau)}{N}, \quad (4)$$

and N is a normalization factor defined by $G(0) = 2$. $g(\tau)$ was fitted using the two-component model with a triplet term

$$g(\tau) = 1 + \frac{1 - f_{\text{triplet}} + f_{\text{triplet}}e^{-\tau/\tau_{\text{triplet}}}}{n(1 - f_{\text{triplet}})} \times \sum_{i=1}^2 f_i \left(1 + \frac{\tau}{\tau_i}\right)^{-1} \left(1 + \frac{\tau}{s^2\tau_i}\right)^{-1/2}, \quad (5)$$

where f_i and τ_i are the fraction and diffusion time of component i , respectively, n is the average number of fluorescent particles in the excitation-detection volume defined

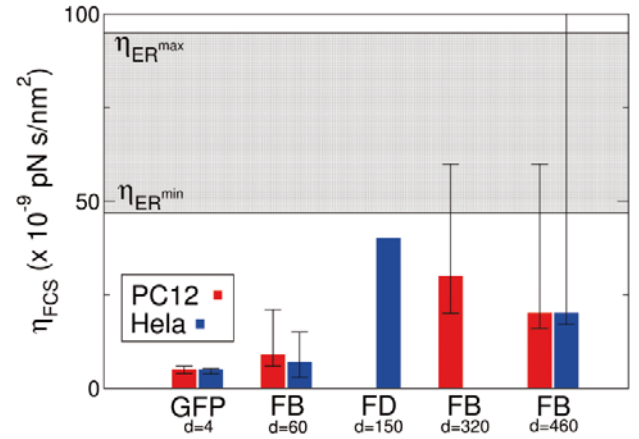


Fig. 7. Viscosity η_{FCS} ($\text{pN s}/\text{nm}^2$) for green fluorescent protein (GFP), fluorescent beads (FB) and fluorescent nanodiamond (FD). η_{FCS} were calculated from diffusion coefficients D shown in table 1 using the equations $D\Gamma = k_{\text{B}}T$ ($T = 25^\circ\text{C}$) and $\Gamma = 6\pi\eta_{\text{FCS}}sr$, where $r = d/2$. The values of $20 \mu\text{m}$ sized PC12 cells (red) were compared with those of $100 \mu\text{m}$ sized HeLa cells (blue). The error bars show the maximum and minimum values of η_{FCS} calculated by using the standard deviations of D (table 1). The ranges of η_{ER} was estimated by using the standard deviation of mitochondrial size r_{m} . Note that the viscosity of water is 1×10^{-9} ($\text{pN s}/\text{nm}^2$) at 25°C .

by the radius w_0 and length $2z_0$, and s is the structure parameter representing the ratio $s = z_0/w_0$. For the 460 nm sized fluorescent beads in the cytosol of the PC12 cell, $g(\tau)$ was fitted by the two-component model whose parameters are $n=12$, $f_1 = 0.25$, $f_2 = 0.75$, $\tau_1 = 1.8 \text{ ms}$, $\tau_2 = 220 \text{ ms}$, $s = 6$, $f_{\text{triplet}}=0.08$ and $\tau_{\text{triplet}} = 10 \mu\text{s}$. Here we fitted our data for the 460 nm sized beads using eq. (5), which may not be regarded as a point-like particle because of their large size, because in a previous study [19], eq. (5) provided the proper value of the diffusion coefficient of 300 nm sized fluorescent beads. Using τ_i obtained by the fitting, the diffusion coefficient D_i was calculated from the published diffusion coefficient for the standard dye (rhodamine-6G) ($D_{\text{Rh6G}} = 280 \mu\text{m}^2/\text{s}$, $\tau_{\text{Rh6G}} = 21 \mu\text{s}$) with the relation

$$\frac{D_i}{D_{\text{Rh6G}}} = \frac{\tau_{\text{Rh6G}}}{\tau_i}. \quad (6)$$

For the 460 nm sized beads in the cytosol, we obtained $D = 0.04 \pm 0.02 \mu\text{m}^2/\text{s}$ from τ_2 . Note that the fast component (τ_1) was an apparent diffusional term caused by blinking of the fluorescent beads [18]. For GFPs and the other beads listed in table 1, we performed the same procedure to obtain D (table 1).

The viscosity of medium η_{FCS} was calculated from diffusion coefficients D using the equations $D\Gamma = k_{\text{B}}T$ ($T = 25^\circ\text{C}$) and $\Gamma = 6\pi\eta_{\text{FCS}}sr$ ($r (= d/2)$ is the radius of a fluorescent probe) (fig. 7). Here we assumed that the beads diffused in the cells mainly due to thermal noise. Figure 7 shows that viscosity values did not significantly depend on cell type ($20 \mu\text{m}$ sized PC12 cells and $100 \mu\text{m}$

sized HeLa cells). Although the viscosity value obtained by using GFPs was regarded as the viscosity of cytosol, which were 5 times larger than that of water [18], the structures inside the cells affected the viscosity for the larger beads. Because the η_{FCS} values for the 150 nm sized nanodiamonds and the 320 nm sized beads were similar to that for the 460 nm sized beads within the accuracy of the measurements, the η_{FCS} value for 1 μm sized beads, which was almost as large as a mitochondrion, was expected to be similar to these values (note that it was difficult to incorporate larger beads, such as 1 μm sized beads, into the 20 μm sized PC12 cells). Because the intervals between filaments in the PC12 cells were approximately 1.5 μm (fig. 2), the effective viscosity reflecting the intracellular structure may converge until the size of the bead is about 1.5 μm .

5 Summary and discussion

We investigated the motion of a 1 μm sized organelle transported at a constant speed by motor proteins. Such an investigation may be important to help elucidate the transport mechanism by multiple motors in future. We measured the power spectrum (fig. 3(b)) and variances of probability distribution ($P(\Delta X)$) of $\Delta X (= X(t + \Delta t) - X(t)$, $X(t)$: the position of an organelle) (fig. 4(b)), and found that the diffusion property was almost normal while diffusion became abnormal when the trajectories included pauses and reversals (fig. 3(b), bottom). When estimating the diffusion coefficient (D_{m}) for the constant drag motion of organelles, we found $D_{\text{m}} \propto 1/\Gamma_{\text{m}}$ (fig. 5) where $\Gamma_{\text{m}} (= 6\pi\eta r_{\text{m}})$ is the friction coefficient. This inverse proportional relationship was similar to that derived from the FDT (the Einstein relation). However, when we compared the viscosity value (η_{ER}) obtained assuming the Einstein relation for the organelle motion, η_{ER} was slightly different from the real viscosity value (η_{FCS}) (fig. 7). This indicates $D_{\text{m}} \neq k_{\text{B}}T/\Gamma_{\text{m}}$.

From the estimated viscosity $\eta_{\text{FCS}} = 2\text{--}4 \times 10^{-8}$ pN s/ nm^2 (fig. 7), the drag force exerted by motor proteins acting on a 1 μm sized organelle, which is driven at a speed of 1 $\mu\text{m}/\text{s}$, is estimated to be approximately 0.3 pN based on the equation $F = 6\pi\eta_{\text{FCS}}\langle r_{\text{m}} \rangle_{\text{s}}\langle v \rangle_{\text{s}}$. The drag force value estimated here is smaller than the reported values for stall forces of kinesin and dynein in cells (about 3 pN for single kinesin and single dynein molecules) [21, 22], which are regarded as the maximum forces that motors can exert. We conclude, therefore, that the drag force value is reasonable. Here, although kinesin and dynein travel in two different directions along a microtubule (fig. 1(a)), the difference in velocities of the two directions for the same mitochondrion was $< 20\%$, indicating that the drag force acting on a mitochondrion did not vary significantly in either direction within the accuracy of the measurement. Therefore, when we analyzed the trajectory $X(t)$, we ignored the direction of mitochondrial movement. The difference in properties ($< 20\%$) of kinesin and dynein cannot be quantified from the averaged drag force values measured here.

From fluorescence observations, the value of the friction coefficient of an organelle is usually difficult to determine precisely, because its exact shape and intracellular viscosity are unknown. When we used the equation $F = 6\pi\eta_{\text{FCS}}\langle r_{\text{m}} \rangle_{\text{s}}\langle v \rangle_{\text{s}}$, we assumed that the shape of an organelle is spherical, (although this is typically not the case) and $\langle r_{\text{m}} \rangle_{\text{s}}$ was approximated from the electron micrographs of organelles shown as cross-sections. If estimation of a drag force is possible only using trajectories, which can easily be measured for any identified organelle based on their specific live staining using fluorescent proteins or fluorescent dyes, such an estimation helps to understand the results of *in vivo* experiments in which physical measurements are really difficult and approximate values are still useful. Noting that the two values (η_{ER} and η_{FCS}) were similar within the range of experimental error bars, and assuming the effect of thermal noise on the constant drag motion of an organelle is large enough, the rough estimation of the drag force can be obtained directly from $X(t)$ shown in fig. 3(a) using the fluctuation theorem (FT) of the form $\ln[P(\Delta X)/P(-\Delta X)] = F\Delta X/k_{\text{B}}T$ (sect. II in Supplementary Material). We obtained $F = 0.5$ pN from the FT.

The number of motors attached to a single organelle is reported to be one to five for dynein and one to four for kinesin. These values are estimated biochemically using quantitative western blotting [23]; however, the number of these motors that actively carry the organelle is still unclear. *In vitro* experiments showed that the number of the active motors can be directly measured through stall force measurements using optical tweezers, and the stall force measurements of a large lipid droplet in a *Drosophila* embryo showed that more than half of the droplets were carried by two kinesins and two dyneins [21, 22]. Because as well as on the stall force distributions, the number of active motors will be considered based on the drag force distributions, it is important to investigate drag forces acting on organelles focusing on their constant drag motion. The results of the present study will serve as a foundation for related future studies on the drag force.

This work was supported by Grants-in-Aid for Scientific Research to K.H. from the MEXT (Nos. 23107703 and 24770143). We thank Prof. H. Noji and Prof. H. Imamura for their help with the experimental design, the members of the Sako Laboratory (RIKEN) for their insightful comments, the members of Sasaki and Ishijima Laboratories (Tohoku Univ.) for providing us with a cooperative research environment, and the staff of BRC (Tohoku Univ.) for assisting us with the transmission electron microscopy measurements.

References

1. S. Ciliberto, S. Joubaud, A. Petrosyan, J. Stat. Mech., P12003 (2010).
2. D. Mizuno, C. Tardin, C.F. Schmidt, F.C. MacKintosh, Science **315**, 370 (2007).

3. S. Toyabe, T. Okamoto, T. Watanabe-Nakayama, H. Take-tani, S. Kudo, E. Muneyuki, *Phys. Rev. Lett.* **104**, 198103 (2010).
4. J. Liphardt, S. Dumont, S.B. Smith, I. Tinoco jr., C. Bustamante, *Science* **296**, 1832 (2002).
5. D. Collin, F. Ritort, C. Jarzynski, S.B. Smith, I. Tinoco jr., C. Bustamante, *Nature* **437**, 231 (2005).
6. A. Alemany, A. Mossa, I. Junier, F. Ritort, *Nat. Phys.* **8**, 688 (2012).
7. K. Hayashi, H. Ueno, R. Iino, H. Noji, *Phys. Rev. Lett.* **104**, 218103 (2010).
8. K. Hayashi, M. Tanigawara, J. Kishikawa, *Biophysics* **8**, 67 (2012).
9. K. Hayashi, R. Hayashi, *Fluct. Noise Lett.* **11**, 124001 (2012).
10. Y. Kim, H. Konno, Y. Sugano, T. Hisabori, *J. Bio. Chem.* **286**, 9071 (2011).
11. E. Usukura, T. Suzuki, S. Furuike, N. Soga, E. Saita, T. Hisabori, K. Kinoshita jr., M. Yoshida M, *J. Bio. Chem.* **287**, 1885 (2012).
12. M. Tanigawara, K.V. Tabata, Y. Ito, J. Ito, R. Watanabe, H. Ueno, M. Ikeguchi, H. Noji, *Biophys. J.* **103**, 970 (2012).
13. Q. Cai, Z. Sheng, *Exp. Neurol.* **218**, 257 (200).
14. S.M.A. Tabei, S. Burov, H.Y. Kim, A. Kuznetsov, T. Huynh, J. Jureller, L.H. Philipson, A.R. Dinner, N.F. Scherer, *Proc. Natl. Acad. Sci. U.S.A.* **110**, 4911 (2013).
15. L.A. Greene, A.S. Tischler, *Proc. Natl. Acad. Sci. U.S.A.* **73**, 2424 (1976).
16. A.J. Hunt, F. Gittes, J. Howard, *Biophys. J.* **67**, 766 (1994).
17. D. Magde, E.L. Elson, W.W. Webb, *Phys. Rev. Lett.* **29**, 705 (1972).
18. C.G. Pack, M.R. Song, E.J. Lee, M. Hiroshima, K.H. Byun, J.S. Kim, Y. Sako, *J. Control Rel.* **163**, 315 (2012).
19. C.L. Kuyper, B.S. Fusimoto, Y. Zhao, P.G. Schiro, D.T. Chiu, *J. Phys. Chem. B* **110**, 24433 (2006).
20. Y.Y. Hui, B. Zhang, Y.C. Chang, C.C. Chang, H.C. Chang, J.H. Hsu, K. Chang, F.H. Chang, *Opt. Express* **18**, 5896 (2010).
21. G.T. Shubeita, S.L. Tran, J. Xu, M. Vershinin, S. Cermelli, S.L. Cotton, M.A. Welte, S.P. Gross, *Cell* **135**, 1098 (2008).
22. C. Leidel, R.A. Longoria, F.M. Gutierrez, G.T. Shubeita, *Biophys. J.* **103**, 492 (2012).
23. A.G. Hendriks, E. Perison, J.L. Ross, H.W. Schroeder III, M. Tokita, E.L.F. Holzbaur, *Curr. Biol.* **20**, 697 (2010).